Desalination and Water Treatment
www.deswater.com

doi: 10.1080/19443994.2014.903867

54 (2015) 2041–2054
May

Taylor & Francis
Taylor & Francis Group

Pineapple leaf (*Ananas comosus*) powder as a biosorbent for the removal of crystal violet from aqueous solution

Shuvee Neupane, S.T. Ramesh, R. Gandhimathi*, P.V. Nidheesh

Department of Civil Engineering, National Institute of Technology, Tiruchirappalli 620015, Tamil Nadu, India, Tel. +91 431 250 3171; Fax: +91 431 250 0133; email: rgmathii@nitt.edu

Received 29 July 2013; Accepted 1 February 2014

ABSTRACT

Dyes are present in the industrial effluents which need to be treated before discharging to the environment as they pose severe environmental and health impacts. For this, biosorption has been considered as an economic and efficient technology as compared to the other treatment processes. Thus, biosorption characteristics of *Ananas comosus* (pineapple) leaf powder (PLP) was investigated for decolorization of crystal violet (CV), a cationic dye from its aqueous solutions employing a batch experimental setup. The parameter studied included contact time, initial dye concentration, adsorbent dose, pH, agitation speed, particle size of adsorbent, and temperature. Different isotherm models, Langmuir, Freundlich, Dubinin–Radushkevich, and Temkin were found. Maximum adsorption was found with <150 µ particle sized 50 mg of PLP at 30˚C with 200 rpm at pH 8. The maximum adsorption capacity (q_m) was found to be 158.73 mg/g. Lagergen pseudo-second-order model best fits the kinetics of adsorption. Intra particle diffusion plot showed boundary layer effect and larger intercepts indicates greater contribution of surface sorption in rate-determining step. Adsorption of CV on adsorbents was found to increase on decreasing initial concentration, increasing pH up to 8, decreasing temperature, increasing agitation speed, and decreasing particle size. Overall, the present findings suggest that PLP is environmentally friendly, efficient, and low-cost biosorbent which is useful for the removal of CV from aqueous media.

Keywords: Biosorption; Crystal violet; Pineapple leaf powder; Isotherms

---

1. Introduction

Synthetic dyes are extensively used in the textile, food, cosmetics, pharmaceuticals, paper, leather, photographic, and aquaculture industries [1]. About 40,000–50,000 tons of dyes are continuously entering the water systems due to improper processing and dying methods from these industries [2]. Color effluents discharged from dye production industries are major concern as they are highly soluble. Due to this they are frequently found in trace quantities in industrial wastewater. The discharge of dye-bearing wastewater into natural streams and rivers possess a severe environmental problem. The entire wastewater may contain elements like sulfur, naphthol, vat dyes, nitrates, acetic acid, soaps, and chromium compounds and heavy metals like copper, arsenic, lead, cadmium, mercury, nickel, and cobalt, and certain auxiliary chemicals all of which collectively make the effluent highly toxic [3]. Highly colored wastes are not only esthetically displeasing but also hinder light

---

*Corresponding author.

penetration and may in consequence disturb biological processes in water bodies [4]. It is therefore necessary to treat these effluents prior to their discharge into the receiving water. However, wastewater containing dyes is very difficult to treat, since the dyes are recalcitrant organic molecules, resistant to aerobic digestion, and are stable to light, heat, and oxidizing agents due to their structure and molecular size [5], and most of the dyes contain aromatic rings [6] which make them mutagenic and carcinogenic [2]; it has also been proven that poor sanitation combined with unhealthy water quality accounts for the largest single cause for disease and death in the world [7].

The present study has been done on adsorption of crystal violet (CV) which is also known as basic violet 3, gentian violet, and methyl violet 10B. Its IUPAC name is N-[4-[bis[4-dimethylamino)-phenyl]-methylene]-2,5-cyclohexadien-1-ylidine]-N-methylmethanaminium chloride (molecular formula $C_{25}H_{30}N_3Cl$ and molecular weight 407.98) and belongs to the class of triarylmethane dyes [2]. CV is being used for various purposes: a biological stain, a dermatological agent, a veterinary medicine, an additive to poultry feed to inhibit propagation of mold, intestinal parasites, and fungus. It is also extensively used in textile dying and paper printing [8]. But CV is toxic to mammalian cells and is a mutagen and a mitotic poison [9]. The dye is responsible for causing moderate eye irritation, causing painful sensitization to light. It can cause permanent injury to the cornea and conjunctiva since the product contains a cationic dye and such dyes have been reported to cause toxicity to mammalian cells [10,11]. It may be absorbed in harmful amounts through the skin and cause skin irritation and digestive tract irritation. In extreme cases it may lead to respiratory and kidney failure, and permanent blindness [2].

Some biological and physical/chemical methods have been employed for removing the dye from industrial effluents, such as coagulation, membrane separation, electrochemical oxidation, ion exchange, chelation by synthetic resin, and adsorption [12]. But these methods possess drawbacks due to their inapplicability to large-scale units along with both energy intensiveness and chemical intensiveness [2]. Also as the dyes are water soluble, stable, and are non biodegradable in nature, they sometimes tend to pass through the conventional treatment methods unaffected. Moreover organic molecules that are not biodegradable, can still be removed from the wastewater by the process of biosorption—the term used to indicate a number of metabolism-independent processes (physical and chemical adsorption, electrostatic interaction, ion exchange, complexation, chelation, and microprecipitation) which takes place essentially in the cell wall rather than oxidation though anaerobic or aerobic metabolism (biodegradation) [13]. Among the pollutants, biosorption is used to remove dyes, phenolics, and pesticides using raw materials which are either abundant (sea weeds), or wastes either from industrial operations (fermentation wastes, activated sludge process wastes) [14–17], or agricultural wastes (banana peels [18], rice straw [19], corncob [20], barley husk [20], papaya seeds [21], orange peels [22], jackfruit peels [23], teak tree bark powder [24], Mangrove bark [25], saw dust [26], wheat shells [27], Borassus aethiopum flower [28], tamarind seed powder [29], hazelnut shell [30], ginger waste [31], watermelon rind [32], and peanut shell [33]). Among these low-cost adsorbents, agricultural biosorbents are abundant in nature, inexpensive, require little processing, and are effective for dye removal [34].

Thus present study investigates the effectiveness of the pineapple leaf powder for the removal of CV from aqueous solution, discusses various mechanisms involved in biosorption, discusses the effects of various parameters such as contact time, adsorbate, and adsorbent concentration, pH, temperature, and agitation speed on biosorption. Pineapple is produced in large quantities in the tropical countries like India, China, Thailand, Malaysia, Taiwan, and Indonesia. Pineapple leaf is a byproduct of the extraction of pineapple fruit. This agricultural waste is suitable for the removal of CV as it is abundant in the country [35]. These natural biosorbents are not only low cost, but also save the disposal cost and prevent the on-site burning. This paper also represents the study of equilibrium and kinetic models used in batch biosorption systems which are important to determine the biosorption capacity of pineapple leaf powder (PLP). As a whole this paper aims to establish PLP as an economic technology for the treatment of dyes in wastewater.

2. Materials and methods

2.1. Biosorbent

Matured pineapple leaves were collected from NIT Tiruchirappalli premises. The leaves were made into small pieces and washed thoroughly with tap water to remove dust, dirt, and other unwanted materials and then dried in the sun to remove moisture. The leaves were oven-dried at 100°C for 48 h. The dried leaves were then ground to fine particles using a grinder. These were then sieved to through 150 μm. The biosorbent was then stored in an air tight container for further use.

2.2. Characterization of biosorbent

The moisture content and the loss on ignition were determined by heating a pre-weighed dry sample (left at 105℃ in an oven and then cooled in desiccators) to 600℃ over a period of 2 h [36]. The point of zero discharge was determined using the solid addition method [37].

2.3. Adsorbate

CV used in this study was of commercial quality and used without purification. The dye stock solution (500 mg/l) was prepared by dissolving accurately weighed quantity of the dye in distilled water. Experimental dye solution of different concentration was prepared by diluting the stock solution with suitable volume of the distilled water.

2.4. Batch studies

Batch biosorbent experiments were carried out in 250 ml conical flasks with 50 ml working volume with a concentration of 10 ppm. A weighed amount (0.05 g) of biosorbent was added to the solution. The flasks were agitated at a constant speed of 150 rpm in an incubator shaker. The influence of pH (2–12), contact time (1–210 min), biosorbent dose (1–70 mg), temperature (30, 40, and 50℃), particle size (<150, 150–300 and >300 μm), and agitation speed (100, 150, and 200 rpm) was evaluated during the present study. Samples were collected from the flasks at predominant time intervals for analyzing the residual dye concentration in the solution. The residual amount of dye in each flask was investigated using UV–vis spectrophotometer. The amount of dye adsorbed per unit of PLP (mg dye per g PLP) was calculated according to the following mass balance equation.

$$q_e = \frac{(c_i - c_e)\,V}{m} \tag{1}$$

The percentage removal of the dye was calculated using the following equation:

$$\text{Percentage removal} = \left(\frac{c_i - c_e}{c_i} \times 100\right)\% \tag{2}$$

where C_i is the initial concentration of the solution and C_e is the concentration at equilibrium.

2.4. Adsorption kinetics

The determination of the biosorption kinetics is an important stage for designing batch biosorption systems. Also in order to select the optimum operating conditions for full-scale batch systems, information on the kinetics of solute uptake is required [38]. In order to investigate the mechanism of adsorption and to determine the rate-controlling step the following kinetic rate equations have been used to test the experimental data.

2.4.1. Pseudo-first-order equation

The pseudo-first-order equation is generally expressed as [39]:

$$\log(q_e - q_t) = \log(q_e) - \frac{k_1}{2.303}t \tag{3}$$

where q_e and q_t are adsorption capacity at equilibrium and at time t, respectively, and k_1 is the rate constant of pseudo-first-order adsorption. The values of log $(q_e - q_t)$ were linearly correlated with t. The plot of log $(q_e - q_t)$ vs. t should give a linear relationship from which k_1 and q_e can be determined as the slope and the intercept, respectively.

2.4.2. Pseudo-second-order equation

The second-order Lagergren equation was given by Ho and McKay [40]. It is expressed as:

$$\left(\frac{t}{q_t}\right) = \frac{l}{k_2\,q_e^2} + \frac{l}{q_e}\,(t) \tag{4}$$

where, k_2 is the rate constant of pseudo-second-order adsorption expressed in g/mg/min.

If the initial adsorption rate h (mg/g/min) is

$$h = k_2\,q_e^2 \tag{5}$$

Then,

$$\frac{1}{q_t} = \frac{1}{h} + \frac{1}{q_e}t \tag{6}$$

The plot of $\frac{t}{q_e}$ and t should give a linear relationship for which q_e and k_2 can be determined as the slope and intercept, respectively.

2.4.3. Intraparticle diffusion

The mechanism of adsorption of a sorbate on a sorbent follows a series of steps. The slowest of these steps control the overall rate of the process. Generally, pore and intraparticle diffusions are often rate-limiting in a batch reactor while, for a continuous flow system, film diffusion is more likely the rate-limiting step [41]. This possibility was tested in terms of a graphical relationship between q_t and the square root of time ($t^{1/2}$), according to the intraparticle diffusion model proposed by Weber and Morris [42]. The intraparticle diffusion model is expressed as

$$q_t = k_{\mathrm{id}} t^{1/2} + C \tag{7}$$

where C is the intercept and k_{id} is the intraparticle diffusion rate constant (mg/g min$^{0.5}$), which can be evaluated from the slope of the linear plot of q_t vs. $t^{1/2}$.

2.4.4. Bangham equation

Kinetic data were further used to interpret the slow step that might have taken place in the present adsorption system [28]. The applicability of the following Bangham equation to present then adsorption of CV onto PLP was tested

$$\log\log\left(\frac{c_0}{c_0 - q_m}\right) = \log\frac{k_0 m}{2.30\,V} + \alpha\log t \tag{8}$$

where C_0 is the initial concentration of the solute in the solution, (mg/l), V is the volume of the solution, (l), m is the weight of the adsorbent used per liter of the solution, (g/l), q is the amount of the adsorbent retained at time t, (mg/g), and α and k_0 are constants.

2.4.5. Boyd plot

The Boyd plot predicts the actual slow step involved in the adsorption process [28]. The Boyd kinetic expression is given by

$$F = 1 - \frac{6}{\pi(22)2} e^{-Bt} \tag{9}$$

$$F = \frac{q_t}{q_0} \tag{10}$$

where q_0 is the amount of CV adsorbed at infinite time (mg/g) and qt represents the amount of dye adsorbed at any time t (min), F represents the fraction of solute adsorbed at any time t, and Bt is a mathematical function of F.

Substituting,

$$1 - F = \frac{6}{\pi(22)2} e^{-Bt} \tag{11}$$

or

$$\mathrm{Bt} = -0.4977 - \ln(1 - \mathrm{F}) \tag{12}$$

The Bt values at different contact times can be calculated using Eq. (12) for various time intervals. The calculated Bt values were plotted against time t.

2.6. Adsorption equilibrium

The data obtained from biosorption experiments are generally represented with equilibrium isotherms. These provided more important parameters for designing and optimizing of the biosorption systems. Different isotherm models can be used to determine the biosorption characteristics of a biosorbent [43]. Equilibrium isotherm model equations such as Langmuir, Freundlich, Temkin, and Dubinin–Radushkevich (D–R) are used to describe experimental adsorption data. It is important to find best-fit isotherm to evaluate the efficacy of the prepared adsorbent to develop suitable industrial adsorption system designs.

2.6.1. Langmuir equation

The Langmuir isotherm is developed by assuming that uniform energies of adsorption onto the surface and no transmigration of adsorbate in the plane of the surface [44]. The Langmuir isotherm may be used when the adsorbent surface is homogenous. The Langmuir isotherm is expressed as [45]:

$$\frac{1}{X/M} = \frac{1}{q_{\max}} + \frac{1}{q_{\max^b}}\frac{1}{c_e} \tag{13}$$

where q_e is the biosorption capacity (mg/g), b is the constant that increases with increasing molecular size, and $q_{\max}$ is the amount adsorbed to form a complete monolayer on the surface (mg/g).

The essential characteristics of the Langmuir isotherm can be expressed by a separation or equilibrium parameter, a dimensionless constant, which is defined by Eq. (14) [46]:

$$R_L = \frac{1}{1 + bc_0} \tag{14}$$

R_L indicates the nature of the adsorption process as given below [47]:

$R_L > 1$	Unfavorable
$R_L = 1$	Linear
$0 < R_L < 1$	Favorable
$R_L = 0$	Irreversible

2.6.2. Freundlich isotherm

Freundlich isotherm model assumes heterogeneous surface energies, in which the energy term in the Langmuir equation varies as a function of the surface coverage [48]. Freundlich isotherm is more accurate by considering an exponential distribution of enthalpies for low coverage of adsorbed species. It is an improvement over Langmuir isotherm by including physical adsorption of species. The equation is a special case for heterogeneous surface species. The Freundlich equation is an empirical equation that is very useful as it accurately describes much adsorption data. The Freundlich equation is expressed as [49]:

$$\log q_e = \log K + \frac{1}{n} \log C \tag{15}$$

where X is the weight of substance adsorbed (mg), M is the weight of adsorbent (g), C is the concentration remaining in the solution, and K and n are the constants depending on temperature, the adsorbent, and the substance to be adsorbed. The coefficients K and n can be estimated from slope and intercept by fitting a line plotting log (X/M) vs. log C.

2.6.3. Dubinin–Radushkevich isotherm

D–R isotherm is another isotherm equation that proposed by Dubinin. He assumed that the characteristics of the sorption curves are related to the porosity of the adsorbent [50]. The linear form of the isotherm can be expressed as follows:

$$\ln q_e = \ln Q_D - B_D\, \varepsilon^2 \tag{16}$$

where Q_D is the theoretical maximum capacity (mol/g), B_D is the D–R model constant (mol^2/kJ^2), and ε is the Polanyi potential and is equal to

$$\varepsilon = \mathrm{RT}\ \ln\left(1 + \frac{1}{c_e}\right) \tag{17}$$

The mean energy of sorption, E (kJ/mol), is calculated by the following equation.

$$E = \frac{1}{\sqrt{2B_D}} \tag{18}$$

2.6.4. Temkin isotherm

The Temkin isotherm equation assumes that the heat of adsorption of all the molecules in layer decreases linearly with coverage due to adsorbent–adsorbate interactions, and that the adsorption is characterized by an uniform distribution of the bonding energies, up to some maximum binding energy [51]. The Temkin isotherm is given as:

$$q_e = B \ln A + B \ln C_e \tag{19}$$

where A (l/g) is the equilibrium binding constant, corresponding to the maximum binding energy, and constant B is related to the heat of adsorption. A plot of q_e vs. ln C_e enables the determination of the isotherm constants B and A from the slope and intercept of the straight line plot.

3. Results and discussion

3.1. Characterization of biosorbent

Table 1 shows some basic properties of PLP. Loss on ignition value is 67% (Table 1) which indicated that the organic content is very high for the biosorbent. Fig. 1 shows the FTIR spectra before and after adsorption for PLP. The point of zero charge of PLP obtained as 6. This shows that at pH less than 6, the surface of the PLP is predominated by positive charges while at pH greater than 6, the surface is predominated by negative charges. As seen in Fig. 1, the band 3,447 cm^{-1} can be ascribed to the hydrogen bonded –OH vibration of the cellulosic structure of PLP. The peak at 2,920 cm^{-1} is due to –CH stretching vibration. The FTIR indicates –N_3 at 2,133 cm^{-1}. The other prominent

Table 1
Properties of PLP

Properties	Values
Specific gravity	1.21
Moisture content	2.9%
Loss on ignition	67%
Point of zero charge	6

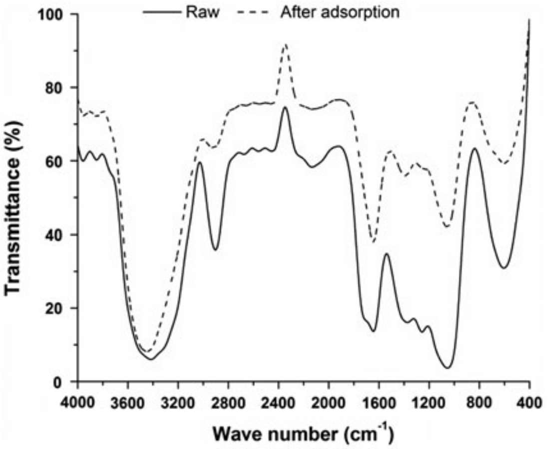

Fig. 1. FTIR spectra for PLP before and after the sorption of CV.

peaks are due to –NH_2 (1,644 cm^{-1}), –NO (1,373 cm^{-1}) [52], and 1,064 cm^{-1} of primary alcohol (C–O) stretching. The adsorbent containing these bends are usually utilized for color removal [29]. From the FTIR analysis, it is clear that some surface functional groups are present on the PLP that might be involved in the dye sorption process.

3.2. Effect of contact time and initial dye concentration

Fig. 2 represents the effect of the initial dye concentration and contact time on CV uptake by PLP. It was observed from Fig. 2 that the uptake was rapid from the first minute itself, slowly the rate decreased and finally reached saturation. This is because of the presence of limited binding or active sites present in the adsorbent. In batch type adsorption system, monolayer of adsorbate (CV) species [53] is formed and the rate of removal of adsorbate species from aqueous solution is controlled primarily by the rate of transport of the adsorbate species from the exterior/outer sites into the interior sites of the adsorbent, PLP particles [54]. Initially there are many active sites, and as the time proceeds the adsorbate binds with the sites and finally every site becomes occupied and there is no further uptake. Thus, the adsorption capacity becomes more or less constant. The equilibrium time was found to be 120 min. Bharathi and Ramesh [32] reported that the equilibrium time to be 180 min for absorption of CV onto watermelon rind. According to OuLL, adsorption equilibrium was achieved within 100 min for 0.1 g of activated charcoal from peanut shell [33]. The equilibrium time for adsorption of CV onto chlor-alkali slurry was found to be 180 min [55]. These results indicate that the attractive force between PLP and CV is higher than that of watermelon rind and chlor-alkali slurry, and comparable with the attractive force of peanut shell.

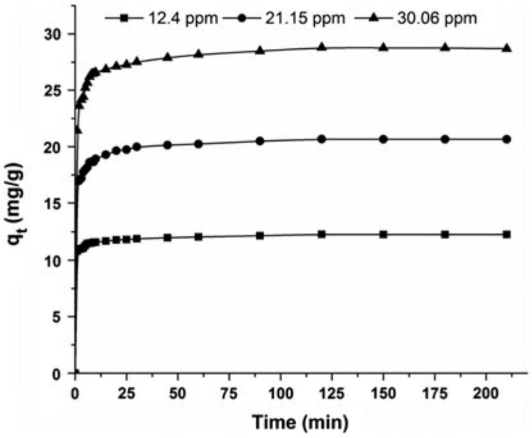

Fig. 2. Effect of initial concentration and contact time on CV uptake of PLP.

From Fig. 2, it can be seen that the adsorption capacity of PLP increases with the increase of initial dye concentration. This is due to increase in concentration gradient which acts as increasing driving force to overcome all mass transfer resistances of the dye molecules between the aqueous and solid phase, leading to an increasing equilibrium sorption until sorbent saturation is achieved [29]. Under the same condition, the percentage of dye removal decreases with the increase in the initial dye concentration. At the lower concentration, all dye molecules interact with the binding sites of the biosorbent, facilitating about 99% adsorption. However, all adsorbents have a limited number of binding sites, which becomes saturated at certain concentration. As such more dye molecules remain unadsorbed in the solution due to the saturation of the binding sites resulting in the decreased removal efficiency [22]. Similar results have been observed for acid yellow-17 removal using *Typha angustata* L. [6], methylene blue onto teak tree bark powder [24], carmoisin onto deoiled soya and bottom ash [56], rhodamine B, fast green and methyelene blue onto red mud [44], and methylene blue onto ground palm karnel coat [57].

3.3. Effect of adsorbent dosage

Equilibrium CV adsorption capacity and removal efficiency profiles of PLP as a function of adsorbent dosage are shown in Fig. 3. The adsorption capacity of PLP decreased with increase in adsorbent dosage. For

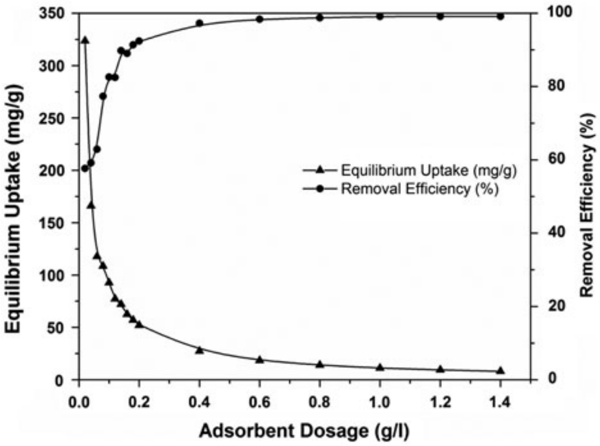

Fig. 3. Effect of PLP dosage on equilibrium CV uptake.

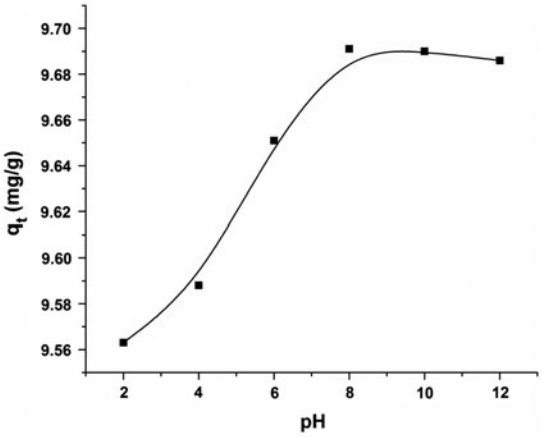

Fig. 4. Effect of solution pH on CV uptake of PLP.

example, with the increase in adsorbent dosage from 0.02 to 0.2 g/l, the adsorption capacity of PLP decreased from 325.65 to 51.88 mg/g. At the same time the CV removal efficiency of PLP increased with increase in dosage. The CV removal efficiency of PLP increased from 57.6 to 92% with the increment of dosage from 0.02 to 0.2 g/l. The increase in CV removal with increase in PLP dosage is mainly due to increase in the volume of active adsorption sites. The decrease in adsorption capacity values of PLP even at higher removal efficiency is mainly due to the excess amount of adsorbent required for the sorption of CV. These values indicate that the quantity of PLP required for the sorption CV is very less. A similar result has been reported by Gandhimathi et al. [17].

3.4. Effect of pH

Aqueous solution pH is a critical parameter as it strongly affects biosorption, surface charge of the adsorbent, the degree of ionization, and the speciation of adsorbate species [58]. Biosorption potential of PLP for CV was seen to increase with increase in solution pH appreciably up to pH 8.0 (Fig. 4). A further increase in solution pH was insignificant. The optimum pH for CV biosorption by PLP was found to be 8.0. CV is a cationic dye, which exists in aqueous solution in the form of positively charged ions. As a charged species, the degree of its sorption onto the biosorbent surface is primarily influenced by the surface charge on the biosorbent, which in turn is influenced by the solution pH. The FTIR spectral analysis indicates the presence of –OH, –CH, and $–NH_2$ functional groups on the PLP surface. At low pH values, the protonation of these surface functional groups easily takes place, and thereby restricts the approach of positively charged dye cations to the surface of the biosorbent resulting in low biosorption of dye in acidic solution. With decrease in acidity of the solution, the surface functional groups become de-protonated resulting in an increase in the negative charge density on the biosorbent surface and facilitating the binding of dye cations. The increase in dye removal capacity at higher pH may also be attributed to the reduction of H^+ ions which compete with dye cations at lower pH for appropriate binding sites on the biosorbent surface. However, with increasing pH, this competition weakens and dye cations replace H^+ ions bound to the biosorbent surface resulting in increased dye uptake.

3.5. Effect of particle size

Adsorption rate of CV dye for three different particle sizes of PLP (<150 μ, 150–300 μ, and > 300 μ) was studied keeping the other parameters as constant. It can be observed from Fig. 5 that as the particle size increases, the adsorption of the dye decreases. This is due to larger surface area that is associated with smaller particles. For larger particles, the diffusion resistance to mass transport is higher and most of the internal surface of the particle may not be utilized for adsorption and consequently, the amount of dye adsorbed is small [30]. Similar trend was observed for adsorption of basic yellow-87 onto two mesoporous materials: MCM41 and carbon aerogel [59], methylene blue onto teak tree bark powder [22], Jordanian diatomite [60], carmoisin onto deoiled soya and bottom ash [56], and rhodamine B, fast green, and methyelene blue onto red mud [44].

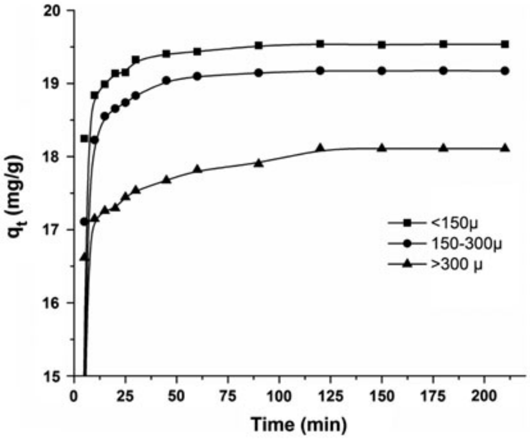

Fig. 5. Effect of PLP size on CV uptake as a function of contact time.

3.6. Effect of agitation speed

The experiments were performed for three agitation speeds 100, 150, and 200 rpm (Fig. 6). It was found that as the agitation speed increases, the biosorption also increases. The mechanism of adsorbate removal involved four steps [29]: (i) migration of adsorbate molecules from the bulk solution to the surface to the surface of the adsorbent; (ii) diffusion through the boundary layer to the surface of adsorbent; (iii) adsorption at a site; and (iv) intraparticle diffusion into the interior of the adsorbent. Increasing agitation speed decreases the boundary layer resistance of the transfer of adsorbate molecules from the bulk solution to the adsorbent surface. Due to this, the adsorbate is forced towards the adsorbent surface and leads to an increase in the diffusion of adsorbate into the surface of the adsorbent [29]. Similar trend was observed for the adsorption of methylene blue onto Jordanian diatomite [60] and teak tree bark powder [22] and CV onto tamarind seed powder [29].

3.7. Effect of temperature

With the increase in the temperature form 30 to 50˚C, the biosorption of CV on PLP decreased from 18.84 to 18.29 mg/g in 5 min (Fig. 7). This may be due to the weakening of the bonds between the dye molecules and the active sites of the biosorbent [61]. Similar trends have been observed in biosorption of lead and cadmium using *Caladium bicolor* biomass [62], rhodamine B, fast green and methyelene blue onto red mud [44], and acid yellow-17 onto *Typha angustata* L. [6]. Taher also reported the similar trend of adsorption of CV on Cassia Siamea, Albizia Labbeck, Nerium Indicum, Durauta Erecta, and Potato Husk [63]. The decrease in the biosorption capacity with the increase in temperature suggests that the process is kinetically controlled by an exothermic process.

3.8. Adsorption kinetics

Five kinetic models (Lagergren's pseudo-first-order and second-order, Intraparticle diffusion, Bangham, and Boyd model) were applied to examine the mechanism of CV removal by PLP (Fig. 8). Experimental and theoretically calculated values for q_e related to the kinetic plots from pseudo-first- and second-order models (Fig. 8(a) and (b)) are given in Table 2. Based on the data, it was found that pseudo-second-order model fitted better than pseudo-first-order model.

Prediction of rate-determining step is important for the design purpose. Generally, for a solid liquid

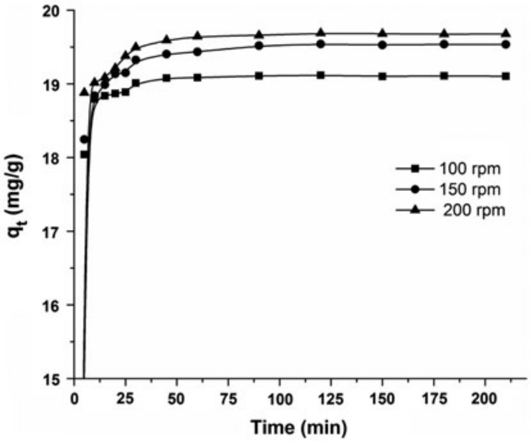

Fig. 6. Effect of agitation speed on CV uptake of PLP as a function of contact time.

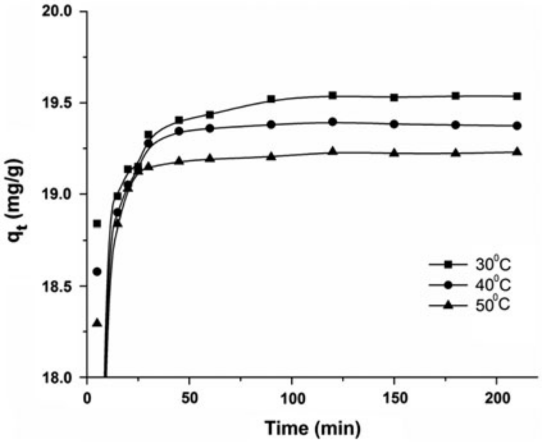

Fig. 7. Effect of solution temperature on CV uptake of PLP.

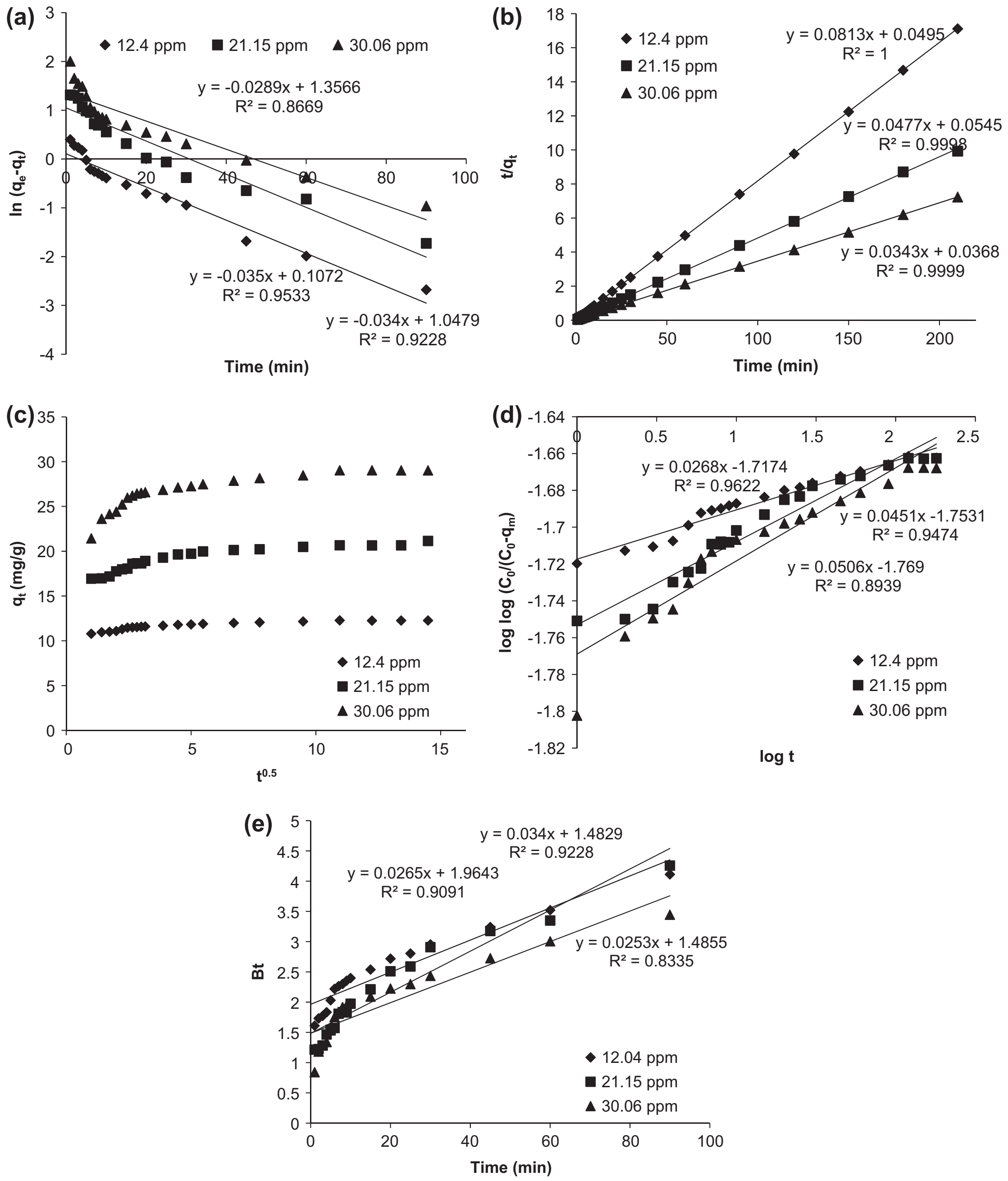

Fig. 8. Kinetics plots of (a) Pseudo-first-order, (b) Pseudo-second-order (c) Intraparticle diffusion model (d) Bangham Model (e) Boyd Plot for CV uptake on PLP at various initial dye concentrations.

adsorption process, the solute transfer is usually characterized by either external mass transfer or intraparticle diffusion or both. The adsorption dynamics can be described by the following three consecutive steps which are as follows [64]:

(1) transport of the solute from bulk solution through liquid film to the adsorbent exterior surface;

(2) solute diffusion into the pore of adsorbent except for a small quantity of sorption on the external surface; parallel to this is the intraparticle transport mechanism of the surface diffusion;

(3) sorption of solute on the interior surfaces of the pores and capillary spaces of the adsorbent.

The sorption of CV onto PLP may be controlled due to film diffusion at earlier stages and as the

Table 2
Variation of the kinetic coefficients with variation in the initial dye concentration

		Pseudo-first-order kinetic model			Pseudo-second-order kinetic model		
CV concentration (ppm)	Theoretical, q_e (mg/g)	q_e (mg/g)	k_1 (1/min)	R^2	q (mg/g)	k_2 (g/mg/min)	R^2
12.4	12.28	1.11	0.08	0.9716	12.3	0.14	1
21.15	21.1	2.85	0.078	0.982	20.96	0.041	0.99
30.7	29.03	3.88	0.066	0.9736	29.15	0.031	0.99

adsorbent particles are loaded with dye ions, the sorption process may be controlled due to intraparticle diffusion. For the adsorption process, the external mass transfer controls the process for the systems that have poor mixing, dilute concentration of adsorbate, small particle sizes of adsorbent, and higher affinity of adsorbate for adsorbent. Whereas, the intraparticle diffusion will control the sorption process for a system with good mixing, large particle sizes of adsorbent, high concentration of adsorbate, and low affinity of adsorbate for adsorbent [28].

From the intraparticle diffusion plot (Fig. 8(c)), it was evident that the adsorption process follows two steps. The first linear portion follows the boundary layer diffusion followed by another linear portion which represents the intraparticle diffusion.

The linearity of the Bangham plot (Fig. 8(d)) shows that the intraparticle diffusion is not the sole process taking place but the boundary layer diffusion also takes place. But it is important to find the slowest step which is the rate-determining step. This can be found by testing the kinetic data with the Boyd plot. The Boyd plot (Fig. 8(e)) is linear and does not pass through the origin suggesting that the external mass transfer mainly governs the rate of the reaction.

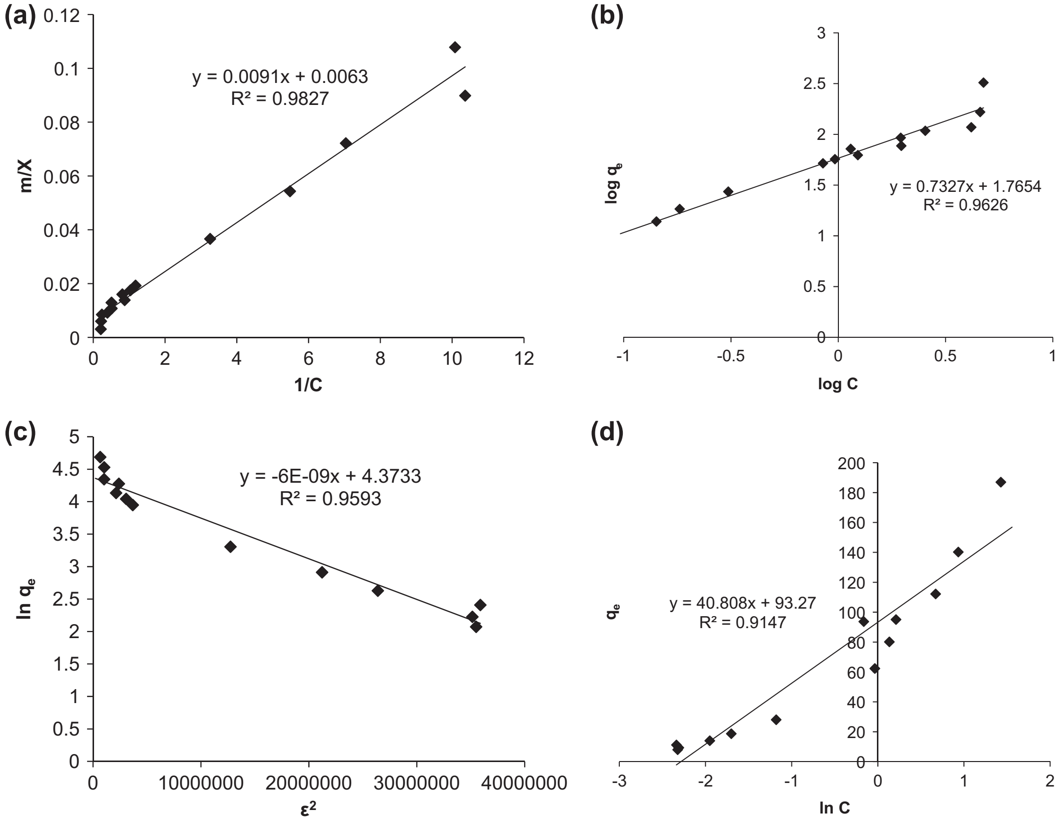

Fig. 9. Plots of (a) Langmuir (b) Freundlich (c) Dubinin–Radushkevich (D–R) (d) Temkin Isotherms for CV uptake on PLP.

3.9. Equilibrium modeling

Equilibrium studies are performed to get the maximum dye adsorption capacities of the adsorbent in the concentration range from 1 to 70 mg/50 ml at 30˚C. The adsorption data were analyzed by the regression analysis to fit the Freundlich, Langmuir, D–R, and Temkin isotherm models (Fig. 9).

The experimental plots and constants (Table 3) clearly indicates that the sorption of CV onto PLP follows Langmuir isotherm depicting that the sorption process is monolayer and homogenous and the sorbate–sorbate interaction is negligible. Also the value of Freundlich constant n is greater than unity thus indicating the favorability of adsorption by the PLP. The maximum fixation is 158.73 mg/g. Since the separation factor $R_L > 0$ (0.10), it suggests that the adsorption is favorable. For R–D isotherm, if the magnitude of E is between 8 and 16 kJ mol^{-1}, the sorption process is supposed to proceed via chemisorptions, while for values of $E < 8$ kJmol^{-1}, the sorption process is of physical nature. The estimated values of E for the present study were found to be greater than 8 kJ mol^{-1} which implies that biosorption of CV on PLP is chemisorptions.

Table 3
Isotherm constants

Isotherm models	Parameters	Values
Langmuir isotherm	q_{max} (mg/g)	158.73
	B (l/mg)	0.69
	R^2	0.98
Freundlich isotherm	K (mg/g)	5.84
	n	1.36
	R^2	0.96
Temkin isotherm	A	9.83
	B	40.808
	R^2	0.91
Dubinin–Radushkevich model	q_m (mg g^{-1})	79.30
	B_D (mmol^2 kJ^{-2})	6×10^{-3}
	E (kJ mol^{-1})	9.12
	R^2	0.96

3.10. Comparison with other low-cost biosorbent

The maximum CV biosorption capacities of various sorbents including PLP were compared (Table 4). The comparison shows that PLP has higher sorption capacity of CV removal than many of the other reported adsorbents. As the biosorbent surface is negatively charged under the experimental conditions, the increasing electrostatic attraction between positively charged adsorbate species and adsorbent particles leads to increased adsorption of CV.

Table 4
Comparison of CV biosorption capacity of PLP with other reported low-cost adsorbents

Sorbents	$q_{\max}$ (mg/g)
Bottom ash [65]	16.13
Raw tendu waste [66]	42.92
Jackfruit leaf powder [67]	43.39
Treated ginger waste [31]	64.93
Teak tree bark powder [4]	142.85
Chaetophora elegans alga [68]	158.7
Tamarind seed [29]	18.35
Mesoporous Mobil Composition of Matter-41 [69]	138.7
Calcined ball clay [70]	65.28
Uncalcined ball clay [70]	77.52
Rice husk carbon [71]	0.41
PLP (Present study)	158.73

3.11. Desorption study

Our previous study on desorption Nidheesh et al. reported that acetic acid is the best eluent for the regeneration of CV adsorbed adsorbent [14]. Therefore, the regeneration of CV sorbed PLP has been carried out using 1 N acetic acid and percent desorption was calculated using [72]:

$$\text{Desorption}\,(\%) = \frac{c_{\text{de}}}{c_{\text{ad}}} \times 100 \tag{20}$$

where c_{de} is the concentrations of CV after desorption and c_{ad} is the concentration of CV adsorbed. 68.5% of PLP regeneration percentage was obtained after the desorption process. This indicates that the CV adsorbed PLP can be used further for the sorption process after desorbing the dyes using acetic acid.

4. Conclusions

The present investigation was undertaken to test the ability of PLP, for the removal of CV from the aqueous solution with equilibrium and kinetic studies. The equilibrium time was found to be 120 min with optimum dose as 1 g/l. Lagergen pseudo-second-order model best fits the kinetics of adsorption. Intraparticle diffusion plot showed boundary layer effect and larger intercepts indicating greater contribution of surface sorption in rate-determining step. Adsorption of CV on adsorbents was found to increase on decreasing initial concentration, increasing pH upto 8, decreasing temperature, increasing agitation speed, and decreasing particle size. Furthermore, this study indicates that the biosorption capacity of the pineapple leaf powder (158.73 mg/g) is better than many other bio and non-bio adsorbents.

Thus, the present study concludes that PLP could be employed as a low-cost and eco-friendly biosorbent as an alternative to the current expensive methods of removing dyes from textile effluents.

References

[1] N.A. Oranusi, A.N. Mbah, Utilization of azo and triphenylmethane dyes as sole source of carbon energy and nitrogen by *bacillus* sp., Afr. J. Appl. Zool. Env. Biol. 7 (2005) 87–94.

[2] A. Mittal, J. Mittal, A. Malviya, D. Kaur, V.K. Gupta, Adsorption of hazardous dye crystal violet from wastewater by waste materials, J. Colloid Interface Sci. 343 (2010) 463–473.

[3] X. Zhang, A. Li, Z. Jiang, Q. Zhang, Adsorption of dyes and phenol from water on resin adsorbents: Effect of adsorbate size and pore size distribution, J. Hazard. Mater. 137 (2006) 1115–1122.

[4] S. Patil, V. Deshmukh, S. Renukdas, N. Patel, Kinetics of adsorption of crystal violet from aqueous solutions using different natural materials, Int. J. Environ. Sci. 1 (6) (2011) 1116–11134.

[5] M.A. Ashraf, M. Hussain, K. Mahmood, A. Wajid, Removal of acid yellow-17 dye from aqueous solution using eco-friendly biosorbent, Desalin. Water Treat. 51 (2013) 4530–4545.

[6] J. Singh, S. Banerjee, D. Gusain, Y.C. Sharma, Equilibrium modelling and thermodynamics of removal of orange g from its aqueous solutions, J. Appl. Sci. Environ. Sanit. 6 (2011) 317–326.

[7] M.A. Ashraf, M.J. Maah, A.K. Qureshi, M. Gharibreza, I. Yusoff, Synthetic polymer composite membrane for the desalination of saline water, Desalin. Water Treat. 51(16–18) (2013) 3650–3661.

[8] A. Adak, M. Bandyopadhyay, A. Pal, Removal of crystal violet dye from wastewater by surfactant-modified alumina, Sep. Purif. Technol. 44 (2005) 139–144.

[9] H.J. Fan, C.S. Lu, W.L. Lee, M.R. Chiou, C.C. Chen, Mechanistic pathways differences between P_{25}-TiO_2 and Pt-TiO_2 mediated CV photodegradation, J. Hazard. Mater. 185 (2011) 227–235.

[10] S.M. Thomas, D.G. MacPhee, Crystal violet: A direct-acting frameshift mutagen whose mutagenicity is enhanced by mammalian metabolism, Mutat. Res. Lett. 140 (1984) 165–167.

[11] J.J. Jones, J.O. Falkinham III, Decolorization of malachite green and crystal violet by waterborne pathogenic mycobacteria, Antimicrob. Agents Chemother. 47 (2003) 2323–2326.

[12] M.A. Ashraf, M.A. Rehman, Y. Alias, I. Yusoff, Removal of Cd(II) onto *Raphanus sativus* peels biomass: Equilibrium, kinetics, and thermodynamics, Desalin. Water Treat. 51 (2013) 4402–4412.

[13] Z. Aksu, Application of biosorption for the removal of organic pollutants: A review, Process Biochem. 40 (2005) 997–1026.

[14] P.V. Nidheesh, R. Gandhimathi, S.T. Ramesh, T.S. Anantha Singh, Adsorption and desorption characteristics of crystal violet in bottom ash column, J. Urban Environ. Eng. 6(1) (2012) 18–29.

[15] P.V. Nidheesh, R. Gandhimathi, S.T. Ramesh, T.S. Anantha Singh, Kinetic analysis of crystal violet adsorption on to bottom ash, Turkish J. Eng. Environ. Sci. 36 (2012) 249–262.

[16] P.V. Nidheesh, R. Gandhimathi, S.T. Ramesh, T.S. Anantha Singh, Modeling of crystal violet adsorption by bottom ash column, Water Environ. Res. 85(6) (2013) 495–502.

[17] R. Gandhimathi, S.T. Ramesh, V. Sindhu, P.V. Nidheesh, Single and tertiary system dye removal from colored textile wastewater using bottom ash: Kinetic and isotherm studies, Iran. J. Energy Environ. 3(1) (2013) 52–62.

[18] M. Achak, A. Hafidi, N. Ouazzani, Sayadi, L. Mandi, Low cost biosorbent "banana peel" for the removal of phenolic compounds from olive mill wastewater: Kinetic and equilibrium studies, J. Hazard. Mater. 166 (2009) 117–125.

[19] B. Hameed, M.I. El-Khaiary, Kinetics and equilibrium studies of malachite green adsorption on rice straw-derived char, J. Hazard. Mater. 153 (2008) 701–708.

[20] T. Robinson, B. Chandran, P. Nigam, Removal of dyes from an artificial textile dye effluent by two agricultural waste residues, corncob and barley husk, Environ. Int. 28 (2002) 29–33.

[21] N. Nasuha, H.Z. Zurainan, H.I. Maarof, N.A. Zubir, N. Amri, Effect of cationic and anionic dye adsorption from aqueous solution by using chemically modified papaya seed, Int. Conf. Environ. Sci. Eng. 8 (2011) 50–54.

[22] G. Annadurai, R. Juang, D. Lee, Use of cellulose-based wastes for adsorption of dyes from aqueous solutions, J. Hazard. Mater. 92 (2002) 263–274.

[23] B.H. Hameed, Removal of cationic dye from aqueous solution using jackfruit peel as non-conventional low-cost adsorbent, J. Hazard. Mater. 162(1) (2009) 344–350.

[24] S. Patil, S. Renukdas, N. Patel, Removal of methylene blue, a basic dye from aqueous solutions by adsorption using teak tree (*Tectona grandis*) bark powder, Int. J. Environ. Sci. 1 (2011) 711–726.

[25] L.S. Tan, K. Jain, C. Rozani, Adsorption of textile dye from aqueous solution on pretreated Mangrove bark, an agricultural waste, J. Appl. Sci. Environ. Sanit. 5 (2010) 284–294.

[26] V.K. Garg, R. Gupta, A.B. Yadav, R. Kumar, Dye removal from aqueous solution by adsorption on treated sawdust, Bioresour. Technol. 89 (2003) 121–124.

[27] Y. Bulut, H. Aydın, A kinetics and thermodynamics study of methylene blue adsorption on wheat shells, Desalination 194 (2006) 259–267.

[28] S. Nethaji, A. Sivasamy, G. Thennarasu, S. Saravanan, Adsorption of malachite green dye onto activated carbon derived from *Borassus aethiopum* flower biomass, J. Hazard. Mater. 181 (2010) 271–280.

[29] H. Patel, R.T. Vashi, Adsorption of crystal violet dye onto tamarind seed powder, E-J. Chem. 7 (2010) 975–984.

[30] M. Dogan, M. Alkan, Adsorption of methylene blue onto hazelnut shell, kinetics, mechanism and activation parameters, J. Hazard. Mater. 162 (2008) 1498–1505.

[31] R. Kumar, R. Ahmad, Biosorption of hazardous crystal violet dye from aqueous solution onto treated ginger waste (TGW), Desalination 265 (2011) 112–118.

[32] K.S. Bharathi, S.T. Ramesh, Biosorption of crystal violet from aqueous solution by *Citrullus lanatus* (watermelon) rind, J. Environ. Res. Develop. 7(1A) (2012) 321–329.

[33] Z.J.X. OuLL, Kinetic, isotherm and thermodynamic studies of the adsorption of crystal violet by activated carbon from peanut shells, Water. Sci. Technol. 67(4) (2013) 737–744.

[34] P. Sharma, H. Kaur, M. Sharma, V. Sahore, A review on applicability of naturally available adsorbents for the removal of hazardous dyes from aqueous waste, Environ. Monit. Assess. 183 (2011) 151–195.

[35] N.A. Lupti, T.H. Yin, Removal of methylene blue using pineapple peel powder as adsorbent, Proceedings of the 3rd CUTSE International Conference 2011, 352–356.

[36] B. Bayat, Comparative study of adsorption properties of Turkish fly ashes: I. The case of nickel(II), copper(II) and zinc(II), J. Hazard. Mater. 95 (2002) 251–273.

[37] N.A. Oladoja, Y.D. Aliu, Snail shell as coagulant aid in the alum precipitation of phases in films on solids, J. Chem. Phys. 12 (2009) 112–113.

[38] S. Salman Ashraf, M.A. Rauf, S. Alhadrami, Degradation of methyl red using fenton's reagent and the effect of various salts, Dyes Pigm. 69 (2006) 74–78.

[39] S. Lagregren, About the theory of so-called adsorption of soluble substances, Kungl. Sven. Veten. Akad. Handl. 24 (1898) 1–39.

[40] Y.S. Ho, G. McKay, Pseudo-second order model for sorption processes, Process. Biochem. 34 (1999) 451–465.

[41] S. Goswami, U.C. Ghosh, Studies on adsorption behavior of Cr(VI) onto synthetic hydrous stannic oxide, Water SA. 31 (2005) 597–602.

[42] W.J. Weber, J.C. Morris, Kinetics of adsorption on carbon from solution, J. Sanit. Eng. Div. 89 (1963) 31–60.

[43] S.T. Akar, A.S. Özcan, T. Akar, A. Özcan, Z. Kaynak, Biosorption of a reactive textile dye from aqueous solutions utilizing an agro-waste, Desalination 249 (2009) 757–761.

[44] V.K. Gupta, I. Suhas, V.K. Ali, Removal of Rhodamine b, fast green, and methylene blue from wastewater using red mud, an aluminum industry waste, Ind. Eng. Chem. Res. 43 (2004) 1740–1747.

[45] I. Langmuir, Chemical reactions at low pressures. 1, J. Am. Chem. Soc. 37 (1915) 1139–1167.

[46] Z. Eren, F.N. Acar, Adsorption of Reactive Black 5 from an aqueous solution: Equilibrium and kinetic studies, Desalination 194 (2006) 1–10.

[47] Z. Aksu, G. Dönmez, A comparative study on the biosorption characteristics of some yeasts for remazol blue reactive dye, Chemosphere 50 (2003) 1075–1083.

[48] T.W. Weber, R.K. Chakravorti, Pore and solid diffusion models for fixed-bed adsorbers, AIChE Journal 20 (1974) 228–238.

[49] H. Freundlich, U¨ ber die adsorption in lo¨sungen [Adsorption in solution], J. Phys. Chem. 57 (1906) 384–470.

[50] M.M. Dubinin, L.V. Radushkevich, The equation of the characteristic curve of the activated charcoal, Proc. Acad. Sci. USSR Phys. Chem. Sect. 55 (1947) 331–337.

[51] M.I. Temkin, V. Pyzhev, Kinetics of ammonia synthesis on promoted iron catalyst, Acta Phys. Chim. USSR 12 (1940) 327–356.

[52] S. Nilratnisakorn, P. Thiravetyan, W. Nakbanpote, Synthetic reactive dye wastewater treatment by narrow-leaved cattail, studied by XRD and FTIR, Asian J. Energy Environ. 9 (2008) 231–252.

[53] G.S. Gupta, G. Prasad, V.N. Singh, Removal of color from wastewater by sorption for water reuse, J. Environ. Sci. Health 23A (1988) 205–217.

[54] K.R. Hall, L.C. Eagleton, A. Acrivos, T. Vermeulen, Pore- and solid-diffusion kinetics in fixed-bed adsorption under constant-pattern conditions, Ind. Eng. Chem. Fund. 5 (1966) 212–223.

[55] R. Jayaraj, A. Suthakaran, S. Amala, C. Anbarasi, S. Selvamathan, P.M.D. Prasath, Competitive adsorption of dyes (crystal violet, methylene blue, malachite green) on chlor-alkali waste (slurry), J. Chem. Pharm. Res. 4(2) (2012) 1251–1258.

[56] V.K. Gupta, A. Mittal, A. Malviya, J. Mittal, Adsorption of carmoisine a from wastewater using waste materials—Bottom ash and deoiled soya, J. Colloid Interface Sci. 335 (2009) 24–33.

[57] N.A. Oladoja, C.O. Aboluwoye, Y.B. Oladimeji, Kinetics and isotherm studies on methylene blue adsorption onto ground palm kernel coat, Turkish J. Eng. Env. Sci. 32 (2008) 303–312.

[58] A. Zubair, H.N. Bhatti, M.A. Hanif, F. Shafqat, Kinetic and equilibrium modeling for Cr(III) and Cr(VI) removal from aqueous solutions by citrus reticulata waste biomass, Water. Air. Soil. Pollut. 191 (2008) 305–318.

[59] X. Wu, K.N. Hui, K.S. Hui, S.K. Lee, W. Zhou, R. Chen, D.H. Hwang, Y.R. Cho, Y.G. Son, Adsorption of basic yellow 87 from aqueous solution onto two different mesoporous adsorbents, Chem. Eng. J. 180 (2012) 91–98.

[60] A. Mohammad, A.M.K. Majeda, N.M.A. Mohammad, A. Stephen, Adsorption behaviour of methylene blue onto Jordanian diatomite: A kinetic study, J. Hazard. Mater. 165 (2009) 589–598.

[61] S. Chowdhury, P. Saha, Sea shell powder as a new adsorbent to remove basic green 4 (malachite green) from aqueous solutions: Equilibrium, kinetic and thermodynamic studies, Chem Eng J. 164 (2010) 168–177.

[62] M. Horsfall Jr, A.I. Spiff, Effects of temperature on the sorption of Pb^{2+} and Cd^{2+} from aqueous solution by *Caladium bicolor* (Wild Cocoyam) biomass, Electron. J. Biotechnol. 8 (2005) 162–169.

[63] A. Taher, M. Mohsin, M. Farooqui, M. Farooqui, Studies on the isotherms, kinetics and thermodynamics of adsorption of crystal violet on low cost materials, J. Adv. Scient. Res. 3(1) (2012) 36–44.

[64] V. Vadivelan, K. Vasanth Kumar, Equilibrium, kinetics, mechanism, and process design for the sorption of methylene blue onto rice husk, J. Colloid Interface Sci. 286 (2005) 90–100.

[65] P.V. Nidheesh, R. Gandhimathi, S.T. Ramesh, T.S. Anantha Singh, Investigation of equilibrium and

thermodynamic parameters of crystal violet adsorption onto bottom ash, J. Int. Environ. Appl. Sci. 6(4) (2011) 461–470.

[66] G.K. Nagda, V.S. Ghole, Utilization of lignocellulosic waste from bidi industry for removal of dye from aqueous solution, Int. J. Environ. Res. 2(4) (2008) 385–390.

[67] P. Saha, S. Chakraborty, S. Chowdhury, Batch and continuous (fixed-bed column) biosorption of crystal violet by *Artocarpus heterophyllus* (jackfruit) leaf powder, Colloids Surf., B: Biointerfaces. 92 (2012) 262–270.

[68] R.S. Rammel, S.A. Zatiti, M.M. El Jama, Biosorption of crystal violet by *Chaetophora elegans* alga, J. Univ. Chem. Technol. Metallur. 46(3) (2011) 283–292.

[69] P. Monash, G. Pugazhenthi, Adsorption of crystal violet dye from aqueous solution using mesoporous materials synthesized at room temperature, Adsorption 15 (2009) 390–405.

[70] P. Monash, R. Niwas, G. Pugazhenthi, Utilization of ball clay adsorbents for the removal of crystal violet dye from aqueous solution, Clean Technol. Environ. Policy 13 (2011) 141–151.

[71] V.K. Verma, A.K. Mishra, Kinetic and isotherm modeling of adsorption of dyes onto rice husk carbon, Global NEST J. 12(2) (2010) 190–196.

[72] I.A.W. Tan, B.H. Hameed, Adsorption isotherms, kinetics, thermodynamics and desorption studies of basic dye on activated carbon derived from oil palm empty fruit bunch, J. Appl. Sci. 10 (2010) 2565–2571.